AIAA SciTech Forum
8-12 January 2024, Orlando, FL
AIAA SCITECH 2024 Forum

10.2514/6.2024-2368

Methods for Mitigating Backsputter in Electric Propulsion Test Facilities II: Beam Halter Demonstration during Hall Thruster Testing

William J. Hurley*, Christopher May†, Grace Zoppi*, Camber Hortop‡, Collin Whittaker*, Tate Gill*, Benjamin A. Jorns§
University of Michigan, Ann Arbor, Michigan, 48109

Seth Thompson¶ and John Williams‖
Colorado State University, Fort Collins, Colorado, 80523

A mitigation strategy for carbon back sputter during testing of a 9 KW class Hall thruster operating at 4.5 KW and discharge voltages of 200 and 300 V is investigated. A beam "halter" consisting of a crossed magnetic and electric field configuration is designed and tested to slow high-energy energy ions before they impact the device's graphite plate. During operation, the halter is operated with magnetic fields ranging from 0 to 115 G while the plate is allowed to electrically float. It is found that the floating potential of the halter increases from 0-40 V and 0-25 V with respect to facility ground for the 300 V and 200 V thruster operating conditions. The thruster cathode to ground voltage varies by less than 3 V, indicating the halter potential is effectively shielded from the thruster discharge. The increase in halter potential thus can decelerate the beam, reducing anticipated backsputter. The degree of reduction in backsputter is quantified with a quartz crystal microbalance mounted in plane with the thruster. It is found that the sputter rates are reduced by approximately 20 % and 38% respectively for the 300 and 200 V conditions. The comparatively improved performance for the 200 V condition is interpreted to be a result of the nonlinear dependence of the sputter yield response to ion energy. The change in floating potential is regressed against a simplified scaling law, which suggests that the electron dynamics may be non-classical in the vicinity of the beam dump. This scaling law is discussed in the context of identifying strategies to improve the efficacy of the halter.

I. Nomenclature

A	=	Area of graphite plate
L	=	Magnetic field length scale
q	=	Fundamental charge
n_e	=	Plasma density in the beam halter
m_e	=	Electron mass
m_i	=	Ion mass
$\dot{m}_{BS}$	=	Mass flow rate of back sputter
u_n	=	Neutral thermal velocity
B_0	=	Magnetic field strength
ω_e	=	Electron cyclotron frequency
ν_c	=	Electron collision frequency
Ω_e	=	Electron hall parameter
c_1	=	Scaling factor for Bohm-like collisions

*Ph.D. Candidate, Department of Aerospace Engineering, Student Member AIAA
†Undergraduate Research Assistant, Department of Aerospace Engineering
‡Masters Student, Department of Aerospace Engineering
§Associate Professor, Department of Aerospace Engineering, Associate Fellow AIAA
¶Ph.D. Candidate, Department of Mechanical Engineering
‖Professor, Department of Mechanical Engineering

c_2 = Scaling factor for electron-nuetral collisions
σ = Electron neutral collision cross section
v_{te} = Electron thermal velocity
j_i = Ion beam current density at the plate
V_b = Average ion voltage
T_e = Electron Temperature
T_i = Ion Temperature
V_{plate} = Plate voltage
V_f = Plate floating voltage
V_d = Discharge Voltage
I_e = electron current to the plate
I = Current to the plate
I_c = Solenoid Current
QCM = Quartz Crystal Micro Balance

II. Introduction

The accurate ground testing of electric propulsion (EP) devices is key to ensuring in-flight reliability and performance. In practice, however, it has been shown that effects relating to the interaction of the thruster with the ground facility can impact testing results. Back sputter is a notable and omnipresent example of such a "facility effect". This process occurs when high-energy ions from the thruster collide with the downstream surfaces in the facility, releasing material. The sputterants, typically graphite due to its comparatively low sputter yield, then migrate back to the thruster, depositing on its surface. The accumulation of of this material can lead to shorting events or potentially obscure erosion of the thruster surfaces. This can call into question the validity of lifetime tests. To date, this problem of back sputter has not precluded the successful development and qualification of EP systems. [1–3] However, for the next-generation of higher power and longer life thrusters, back sputter will only increase in magnitude. This process thus poses a major challenge for the testing of high power concepts. [4]

The goal of this two part work is to explore a novel strategy for reducing and potentially eliminating backsputter during thruster testing. The "beam halter" concept is based on using a crossed-field plasma, conformally similar to a Hall effect thruster, to decelerate ions emitted from a thruster to energies below the sputter rate of the walls in the chamber. In part I of this study, we investigated a prototype of the concept on a small scale gridded ion thruster and parametrically characterized its operation.[5] The results from this preceding study indicated that this is a viable concept. In Part II of this work, we explore a larger scale version of this idea operating in conjunction with a moderately-powered Hall thruster.

This paper is organized as follows. In the third section, we overview the theory of operation of the beam halter. In the fourth section, we describe the design and construction of the device. In the fifth section, we outline the experimental setup including the Hall thruster, facility, operational methodology, and diagnostics we used to characterize the halter's operation. Finally, we present the results from the experiment and discuss the key findings.

III. Theory of Operation

Fig. 1 shows a diagram of the beam halter principle of operation. It consists of a planar geometry with a magnetic field, B_0, applied transverse to a graphite plate. The plate's normal is oriented toward the quasi-neutral ion beam with energy V_b originating from the thruster. As the plasma approaches the beam halter, the transverse magnetic field impedes electron motion to the graphite plate due to the electrons' small mass. Since the electrons are trapped in the magnetic field, the initial flux of ions to the plate is greater than the electron flux, which increases the voltage of the plate. The growing voltage at the plate produces an electric field, E, to retard the ion motion so that the electron and ion flux are balanced. Ideally, the energy of the ions is reduced below the sputtering threshold of graphite (e.g. $\sim$ 30 V for xenon [6]) so that back sputter is eliminated.

A key feature of the halter is that by design, the the electric field that arises to reduce the ion energy is confined to the region of strong tranverse magnetic field. This is ensured by a consideration of a generalized Ohm's law (neglecting

pressure effects) for electron momentum

$$I_e = AE\frac{q^2 n_e}{m_e}\frac{\nu_c}{\omega_e^2 + \nu_c^2}, \tag{1}$$

where A is the area of the plate, L is the effective extent of the magnetic field in the direction normal to the plate, q is the fundamental charge, m_e is the electron mass, ω_e is the electron cyclotron frequency, n_e denotes the electron density, and ν_c is the electron collision frequency. This result shows that for a given electron current, the electric field will be maximized and localized to the region of peak magnetic field, i.e where the effective impedance to cross-field electron motion is the greatest.

This localizing of the electric field is a critical consideration. Absent this effect, any electric field that arises from the plate in principle will be able to interact with the main plume, potentially changing the electrical characteristics of the main discharge. Indeed, this was observed in previous tests of adjusting the downstream electrical potential of non-magnetically isolated beam dumps in Hall thruster tests. [7] Therefore, the beam halter must have a sufficiently strong transverse magnetic field to impede electron flux. As a corollary, intuitively, we would anticipate the collection voltage and thus effective electric field to increase with a stronger magnetic barrier.

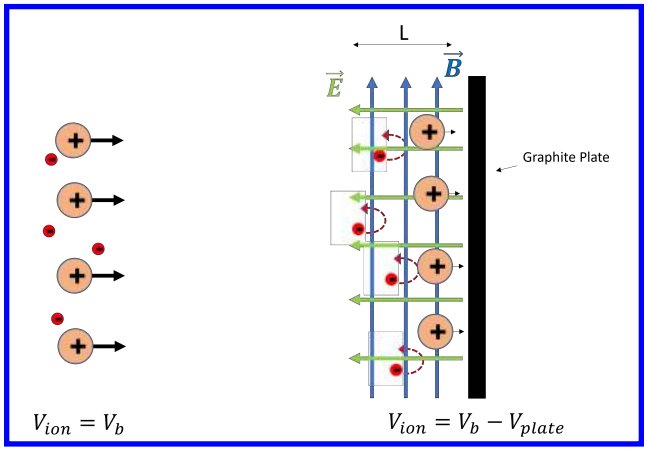

Fig. 1 Representative figure of the beam halter operation. The transverse field impedes electrons, and the plate voltage (floating or biased) slows down beam ions.

With this in mind, we can motivate based on the analysis provided in our accompanying paper [5] how the floating potential should respond to magnetic field. To that end, we quote the result from this previous study for the anticipated current to the halter:

$$I = A\left(-\frac{V_{plate}}{L}\frac{q^2 n_e}{m_e}\frac{\nu_c}{\omega_e^2 + \nu_c^2} + \frac{1}{2}j_i\left(1 + erf\left[\sqrt{V_b/T_i} - \sqrt{V_{plate}/T_i}\right]\right)\right), \tag{2}$$

where we have V_b is the ion voltage in the beam referenced with respect to ground, V_{plate} is the bias of the plate referenced with respect to ground, T_i is the ion temperature, j_i is the current density of the ion beam incident on the plate. The plasma quantities represent averages across the region where the magnetic field is finite (distance L from the surface). This formulation assumes that the electron current across the halter's field is governed by a simplified Ohm's law (first term) neglecting pressure terms, and the ion flux to the plate is kinetic and collisionless with the momentum retarded by the plate voltage (second term). This latter term is based on the same result inferred from retarding potential analyzer theory. [8] The expression in Eq. 2 also assumes that the plasma potential of the beam is approximately at ground potential, i.e. 0 V.

We can extract an analytical scaling law for the floating voltage from Eq. 2 by assuming the current, $I = 0$, and invoking a series of simplifying expressions. First, we consider the case where the magnetic field adjacent to the beam dump is sufficiently strong that the Hall parameter, $\Omega_e = \omega_e/\nu_c \gg 1$. Second, we assume that the floating voltage is below the beam potential, $V_{plate} \ll V_b$, such that the ion current remains approximately constant with V_{plate}. This is justified later by the magnitudes we observe from our experimental measurement. Third, we account for the fact that the density, n_e, inside the beam halter magnetic field will be higher than the density of the flow from the thruster

before entering the magnetic field. This stems from the fact that the beam is slowed electrostatically. We can invoke ion continuity, under the assumption of negligible ionization, to approximate this scaling as

$$n_e = \frac{j_i}{q\sqrt{\frac{2q}{m_i}(V_b - V_{plate})}} \tag{3}$$

where m_i denotes the ion mass. Armed with these assumptions, Eq. 2 can be simplified to an expression that depends on the floating potential of the beam dump referenced with respect to ground:

$$V_f = \frac{1}{2}\frac{q}{m_i}(LB_0\Omega_e)^2\left[-1+\sqrt{1+4V_b\frac{m_i}{q}(LB_0\Omega_e)^{-2}}\right] \tag{4}$$

Eq. 4 illustrates how the anticipated floating potential scales with the plasma properties and design considerations of the beam dump. We immediately see that as the Hall parameter and magnetic field are increased, the floating potential will increase. Physically, this stems from the fact that the effective barrier to electron motion across the magnetic field lines increases, reducing electron motion to the plate. The electric field must rise to draw additional electrons across the field lines to ensure a zero-current condition. We also see that the characteristic length of the magnetic field can influence the floating potential. This stems from the approximation that the electric field is uniform across the magnetic field with $E = V_f/L$. Therefore, longer magnetic field lengths impede electron motion more which drives higher floating potentials.

In practice, the actual floating potential will be a strong function of the effective collision frequency of electrons in the halter. These can be influenced by non-classical effects and non-ideal geometries (e.g. field lines that intercept rather than run tranverse to the halter). We consider in the discussion multiple models for this transport in the context of our experimental measurement.

IV. Beam Halter Design

Armed with the guidance from the previous section that a strong transverse magnetic field is a critical driving factor for the efficacy of the halter, we describe here the prototype beam halter we employed for operation in conjunction with a Hall thruster. We note here that in a departure from the smaller scale prototype investigated in Part I, we adopted an electromagnetic configuration without ferromagnetic material to generate our transverse field. This decision was motivated by the need to generate a much larger area of magnetic structure in order to subtend the beam of a Hall thruster, and the desire to be able to parametrically investigate the role of changing magnetic field strength.

Fig. 2 shows a three-quarters drawing of the prototype. The configuration consists of a 0.6 m x 0.6 m graphite panel mounted inside three pill-shaped solenoids. Each solenoid has an average width of 28 cm and a length of 66 cm and employs 600 turns of 14 gauge polyamide-imide coated wire. The spacing between solenoids was approximately 29 cm. All three surfaces of the solenoids facing the plasma beam were covered with graphite felt. We note here that the middle solenoid was necessary to help ensure magnetic field uniformity and strength along the graphite plate, but its presence reduces the efficacy of the beam Halter. This surface is not electrically biased and thus cannot in principle slow ions. This places an upperbound on the reduction in sputtering we anticipate based on the relative area of this solenoid compared to the plate of ~ 93 %. In practice, we found reductions in sputtering did not achieve this level in this proof of concept.

We performed a series of simulations in order to evaluate the anticipated shape and strength of the magnetic field produced by this solenoid configuration with respect to the graphite plate. To this end, we used the AC/DC module in COMSOL Multiphysics with a coil current of 5 A. Each solenoid was modeled as a homogenized multi-turn conductor with 3000 Amp turns (600 turns of 5 A). Fig. 3(a) shows a top-down view of the transverse magnetic field strength extracted from the mid-plane of the geometry. This plot illustrates that we were able to achieve relatively uniform field strength for a distance of up to 10 cm from the halter with magnitudes exceed 90 G at 5 A. Significantly as well, the magnitude of the magnetic field drops precipitously to zero outside the solenoids, thus ensuring the halter will not perturb the downstream magnetic field of the thruster. Fig. 3(b) shows select magnetic field streamlines from the simulation where we see that the field is primarily transverse to the plate inside the beam halter. Fig. 3(c) shows a plot of the average transverse magnetic field strength in the 10 cm region adjacent to the graphite plate as a function of coil current. As can be seen, the magnetic field is linear with the input current, exceeding 100 G at 6 A. This latter current is the maximum we employed for this test.

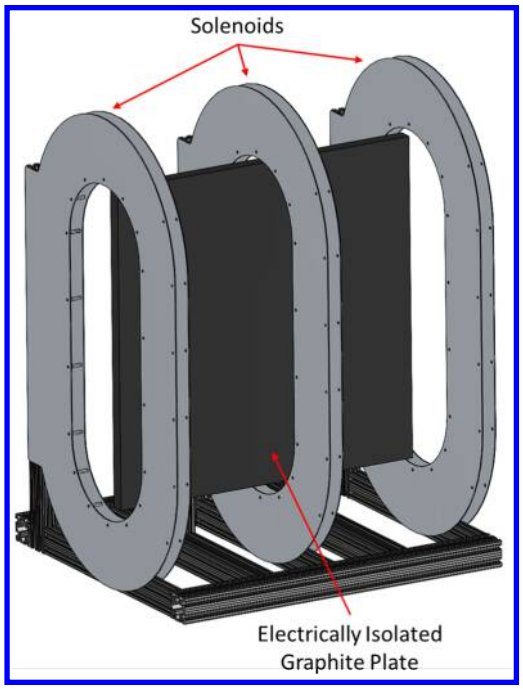

Fig. 2 Beam Halter assembly.

V. Experimental Setup

We used the H9 Hall thruster as the ion source for this proof of concept of the halter. This device is a 9 kW class magnetically shielded laboratory Hall thruster developed jointly by the Jet Propulsion Laboratory, the University of Michigan, and the Air Force Research Laboratory. [9, 10] It is intended as a common research test article for investigating the physics and engineering of Hall thrusters. As described in Ref. [9], the H9 employs a centrally mounted lanthanum hexaboride (Lab6) cathode. The discharge chamber is made of boron nitride, the anode is comprised of stainless steel, and there are two graphite pole covers that protect the thruster poles. The magnetic circuit utilizes a "magnetically shielded" field topology [11, 12] to reduce energetic ion bombardment of the walls. The nominal discharge current of the H9 is 15 A, with discharge voltages from 200 V to 600 V. In this study, we operated the thruster on krypton gas at 200 V and 300 V discharge voltage and 15 A with a 7% flow split to the hollow cathode. All testing was performed in the Alec D. Gallimore Large Vacuum Test Facility (LVTF), a 6 m diameter by 9 m steel chamber with 17 cryopumps [13]. The facility has a nominal pumping speed of 600,000 L/s on krypton. At 300 V, 15 A with the H9 on krypton, the nominal in-plane background pressure was measured at 7 μTorr-Kr by a calibrated Stabil ion gauge mounted in the same plane as the thruster with its aperture facing downstream.

Fig. 4 shows a top-down schematic of the relative orientation of the thruster with respect to the halter as well as relevant diagnostics. The thruster was centrally mounted in the chamber while the beam halter was positioned at a distance of 2.5 thruster diameters downstream. This relative spacing ensured the halter subtended approximately 60% of the thruster ion beam (based on previous far-field probe measurements of the divergence [14]).

During operation, we increased the current to the coils in the solenoids while monitoring the beam dump floating potential, the cathode to ground voltage, and the backsputter rates from the facility. We use the cathode-to-ground voltage as a metric for the impact of the beam halter on the thruster's electrical configuration. This parameter is an indication of the change in potential difference between the thruster's near-field plume and the facility ground (c.f. Ref. [15]). If this value remains invariant in the presence of the beam halter, it is a qualitative indication that this device is not changing the near-field plasma of the thruster.

We characterized the backsputter by employing a quartz crystal microbalance (QCM) with an Inficon XTC/3 controller. We mounted the QCM ~ 0.6 m away from the center of the thruster in a position to ensure that we were capturing the back sputter from the graphite plate. We note here that the QCM measurements can be highly sensitive to thermal variations. We employed both active cooling and a radiation shield to mitigate this effect but ultimately found that the temperature would fluctuate. We suspect this may in part be attibuted to heat reflected from the halter. We quantified the uncertainty introduced by these temperature fluctuations by measuring the deposition rate for a given

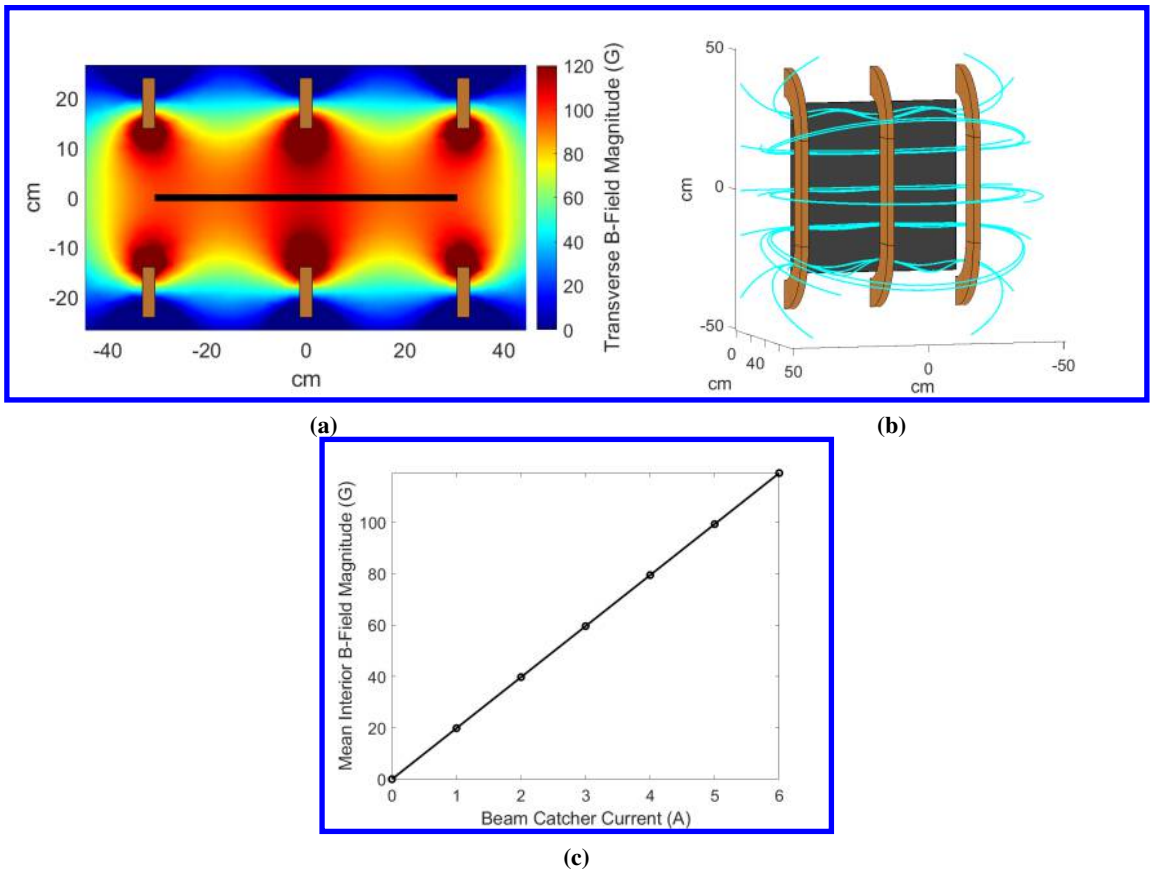

Fig. 3 (a) Top-down simulation of transverse B-field component strength as a function of position at a coil current of 5 A. The trace is extracted from the mid-plane bisecting the halter. (b) Plot of select 3D streamlines from the simulation. (c) Average transverse field strength as a function of coil current.

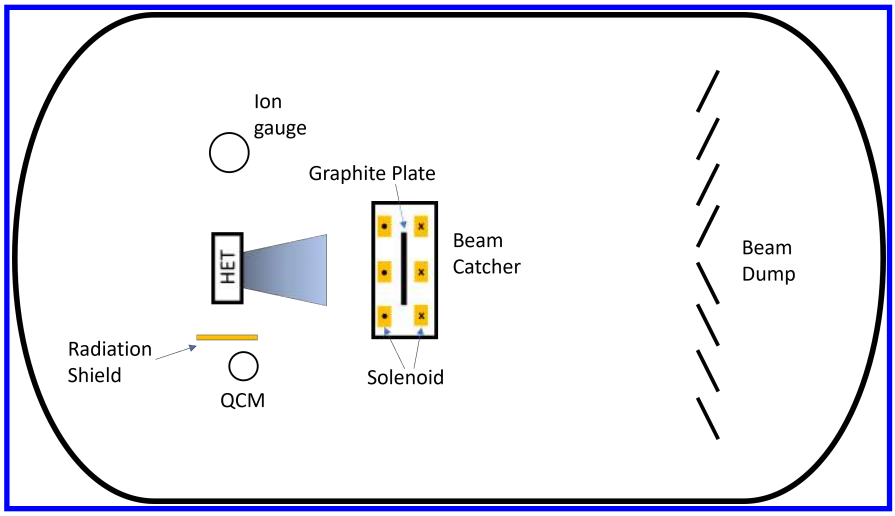

Fig. 4 Top-down view of the experimental setup up in LVTF. Included are the notional positions of the thruster, beam halter, QCM, and ion gauge.

operation condition over a 5-10 minute period. We ultimately found that even though the QCM temperature would change by 1-3 degrees, the reported deposition rate remained constant.

VI. Results

In this section, we present the results from testing of the beam halter. We first show photos capturing qualitative behavior in response to different field strengths. We then show results for the measured potentials and sputtering rates as a function of applied field strength.

A. Images

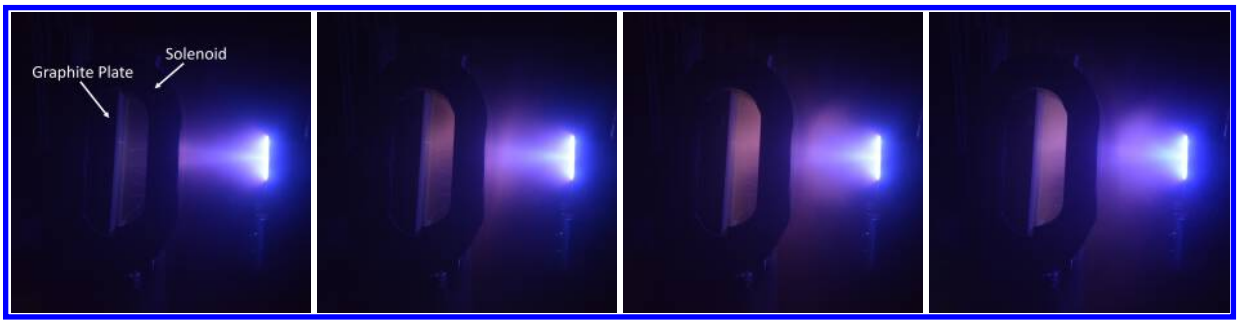

Fig. 5 Images with the same camera settings of the operation of the beam halter with a coil current of a) 0 A, b) 2 A, c) 4 A, and d) 6 A. The Hall thruster is operated on krypton at 200 V discharge voltage and 15 A discharge current.

Fig. 5 shows the beam halter at different solenoid currents for the 200 V and 15 A operating condition. We draw attention to two salient qualitative features from these results. First, we see that as the solenoid current (magnetic field strength) increases, there is an enhanced intensity of purple glow in the gap between the solenoid and plate. Purple light emission qualitatively is associated with excitation of krypton neutrals in these devices. As such, we hypothesize that the increasing intensity of glow may be attributed to enhanced confinement of electrons in this gap which induces a higher rate of neutral excitation. To this point, regardless of magnetic field strength, since the ions are sufficiently massive to remain unmagnetized, we anticipate that the same flux of ions from the thruster will impinge and recombine on the graphite plate, giving rise to a local increase in neutral density adjacent to the beam dump. We would anticipate approximately that the local neutral density would scale as $n_n = (j_i/(qu_n))$where u_n is the neutral speed of the neutrals reflecting from the halter. Assuming room temperature for the reflect ions, we might expect local pressures as high as 20 uTorr, which is a factor of three higher than the ambient pressure. The increasing field strength does impede the motion of electrons, presumably raising their local density and residence time. With increasing coil current then, the probability of electrons inducing excitation of the high density neutral gas increases, leading to a higher degree of excitation and a brighter glow.

The second feature we note is that the glow in the gap appears to be partially asymmetric with a more intense region toward the top of the photos. This asymmetry is in the same direction as the anticipated $E \times B$ drift. We suspect then that the asymmetry is in part driven by the fact that electrons are preferentially driven to drift upward where they impact ionize the gas. Taken together, these two observations qualitatively support the idea that the beam halter is confining electrons. In the next section we turn to quantifying this effect.

B. Potential measurements

Fig. 6 shows results of the cathode to ground voltage and floating voltage referenced with respect to ground as a with the thruster at 200 V and 300 V as a function of coil current to the solenoids. As can be seen, the cathode potential did vary moderately with a change on the order of 1-4 V as the magnetic field of the solenoid changed. This variation could be a qualitative indication that the dynamics of the beam halter are influencing the plume of the thruster. However, we note that these changes are minor compared to variations in the beam dump potential ($< 10\%$), which suggests in turn that although the thruster is not perfectly shielded from the beam halter, the relative impact is moderate. As a corollary, we can assume that changes in the far field plume potential, which are typically on the order of the ground potential (0) are also variant with magnetic field strength.

With this in mind, we see from Fig. 6(b) that the floating potential for both operating conditions monotonically increases with respect to facility ground as a function of solenoid current. This trend is broadly consistent with the

scaling argument presented in Eq.‘4 and would suggest that electron confinement is in fact increasing with magnetic field strength. Moreover, subject to the assumption that the far-field plasma potential remains relatively unchanged with beam current, the increase in the halter potential indicates that this device is providing an electric field to retard ion motion. The maximum retarding potential with 300 V is 40 V while it is 26 V for the 200 V condition. While these potentials are well-below the beam energy (a result we return to in Sec. VII.C), they still suggest that the ion energy incident on the plate should be reduced. This would be manifest as a reduction in sputtering yield. We explore this possibility in the following section.

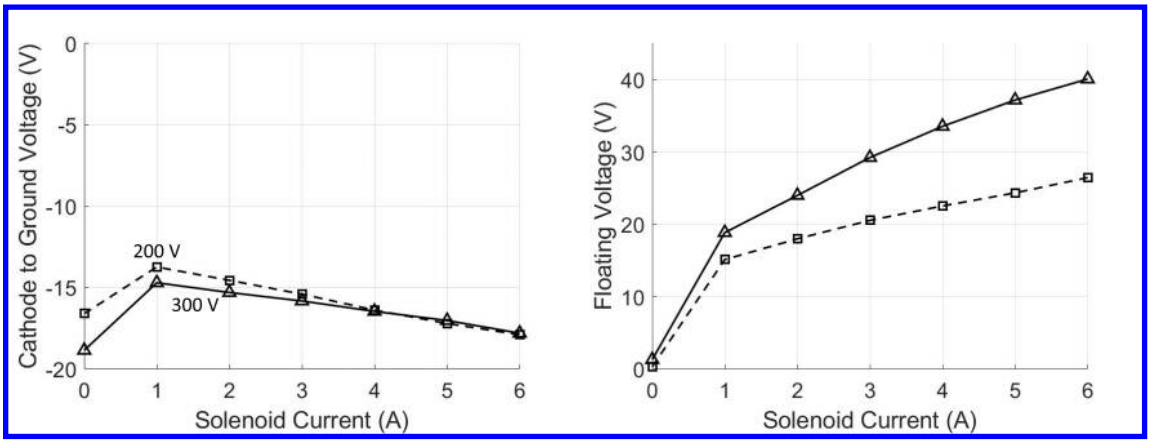

(a) **(b)**

Fig. 6 (a) Cathode to ground voltage and (b) floating voltage of the graphite plate with respect to ground as a function of solenoid current with the thruster operating at 300 V and 200 V and 15 A discharge current.

C. Backsputter measurements

In Fig. 7 we plot the deposition rate measured by the QCM for both discharge voltages as a function of solenoid current. As can be seen, the back sputter rate decreases in each case with increasing field strength. The rates of reduction qualitatively mirror the increase in floating potential shown in Fig. 6. This is consistent with the interpretation that the halter is reducing ion energy and therefore lowering the effective sputtering rate from the surface. The rate of reduction improves with higher retarding potentials (higher coil currents). The maximum decrease is from approximately 16 um/kh to 13 um/kh for the 300 V case– a 20% reduction— and from 4 um/kh to 2.5 um/kh for the 200 V case— a 38% reduction. The fact that there is more pronounced reduction for the 200 V condition likely can be explained by the non-linear response of the sputtering curve–a point we return to in the discussion. Overall, the sputter rate for the 200 V condition is a factor of three lower than the 300 V case, stemming from the lower energy and ion flux at this condition. Taken together, these results provide a positive proof of concept that this method can work, though it remains far from entirely mitigating backsputter.

VII. Discussion

We discuss in the following key results and implications of those results. We first discuss why the 200 V case exhibited an improvement in sputtering reduction over the 300 V case. We then leverage the scaling laws presented in Eq. 4 to regress our data and gain insight into the limitations of our approach. We conclude with a discussion of possible strategies to improve the halter effectiveness.

A. Comparison of reduction in sputtering from 200 V and 300 V conditions

As discussed in the context of Fig. 7, it is evident from our results that the percentage reduction in sputter yield for the 200 V case is greater than the reduction for the 300 V case. This may be understood qualitatively by considering a

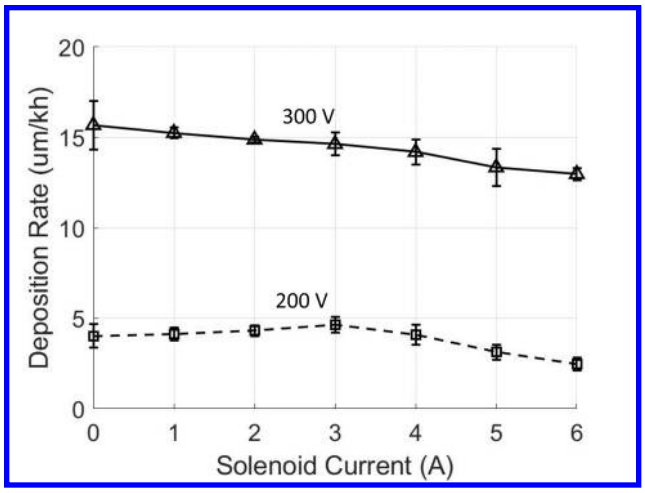

Fig. 7 Deposition rates measured by the QCM as a function of coil current.

simplified model for sputter rate normalized by the 300 V and 0 G magnetic field condition:

$$\dot{m}_{BS}(V_d, I_c) = \dot{m}_{BS}(300V, 0A)\frac{Y(E(V_d, I_c))}{Y(E(300V, 0))} \tag{5}$$

where V_d denotes the discharge voltage, $\dot{m}_{BS}$ is the back sputter mass flow rate, Y() is the sputtering yield, $E(V_d, I_c)$ denotes the ion energy at the halter graphite plate when the thruster is at discharge voltage V_d with halter solenoid current of I_c. We have assumed in this formulation that the current density is constant among cases, which stems from the fact that the discharge current is maintained at the same level. Eq. 5 shows that the anticipated backsputter rate scales as the ratio of the sputter yield from the normalized condition compared to the present condition. For many materials such as graphite [16], the sputter yield from noble gases is a monotonic function of ion energy. However, at sufficiently large incident energies, e.g. > 200 V, the rate of increase with energy changes inflection and becomes more shallow. The implication is that fractional changes at lower incident energy can have a more pronounced change in sputtering yield than the same fractional change in energy at higher values.

This type of dependence may explain the relative rate changes exhibited by our results. Indeed, overall, the sputtering from 200 V is lower than 300 V, reflecting the fact that sputtering yield at these lower incident energies is reduced. However, the fractional change in energy with coil current between the 200 V and 300 V cases due to retardation from the beam halter is approximately the same (25 V/200 V versus 40 V/300 V). In light of the nonlinear dependence of sputter yield on energy, this may explain why there are fractionally more gains in reducing sputter at the 200 V condition.

B. Comparison to Theory

As outlined in Sec. VI and shown in Fig. 6(b), although the beam halter does support an increase in retarding potential, the magnitude is not high enough to be commensurate with the beam energy. Qualitatively, in light of Eq. 4, this result would suggest that the confinement of electrons is curtailed, i.e. there are mechanisms such as collisions allowing for cross-field electron motion. We discuss possible mechanisms driving this process in the following.

To this end, we compare the experimental floating voltage shown in Fig. 6b to that predicted by the theory (eq. 4). To close the equation, we must assume a form for the electron collision frequency. We try two different formulations of the electron collision frequency in this analysis. In the first form, we assume that the electron motion transport is governed by Bohm diffusion. This can be written as

$$\nu_c = c_1\omega_c, \tag{6}$$

where ν_c is the collision frequency, ω_c is the cyclotron frequency, and c_1 is a scaling constant. In the second form of the collision frequency, we assume classical electron-neutral collisions dominate. This is in part motivated by the large amount of neutral excitation exhibited in Fig. 5 and our back of the envelope calculation suggesting pressures may be over five times ambient at this plate. The form for this electron-neutral collision frequency is written as

$$\nu_c = c_2 n_n \sigma(T_e) v_{te} \tag{7}$$

where $\sigma(T_e)$ is the cross-section for collision, v_{te} denotes the electron thermal speed, n_n is the neutral density, and c_2 is a scaling factor. For this analysis we assume the electron temperature in the plume is 1 eV, and the neutral density is given by $n_n = j_i/(qu_n)$, where u_n is the neutral thermal velocity. This formulation for the neutral density assumes that all ions that collide with the plate recombine and are reflected at the thermal velocity. For each form of the collision frequency, we tune the parameters c_1 and c_2 so that the predicted plate floating voltage at a solenoid current of 5 A matches the experimental data. We plot the predicted floating voltage against the experimental data in Fig. 8.

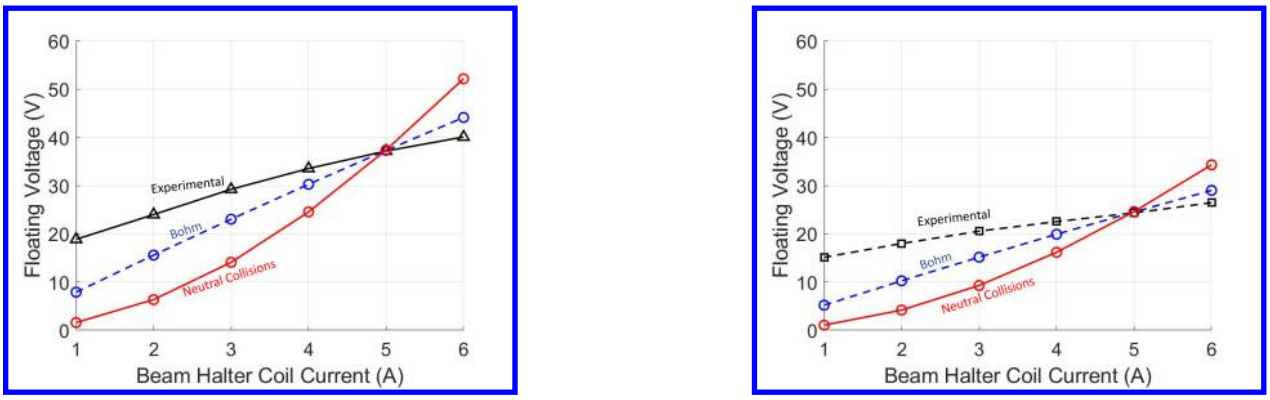

(a) **(b)**

Fig. 8 Predicted floating voltage for the plate as a function of solenoid current at a thruster discharge voltage of a) 300 V, and b) 200 V.

From these comparisons, we see that the effect of the assumed collisions–either Bohm-like or classical–is to reduce the effective floating voltage. This effect in turn is mitigated by increasing the magnetic field. Qualitatively, the experimental response of the beam voltage to solenoid current is more consistent with the Bohm-like scaling. Both exhibit linear-like dependence over this magnetic field range. This may qualitatively suggest that the transport is non-classical in the transverse region of the halter. This conclusion has the caveat, however, that our analysis does not consider other geometric factors that could also adversely impact confinement such as the ability of some magnetic field lines from the solenoid to terminate on the graphite panel (therefore allowing for enhanced electron current along field lines). Alternatively, our geometry is planar and therefore the electron drifts are not closed. This could serve as another loss process. Taken together, these effects could be manifest as approximate reductions in the Hall parameter–potentially in a way that better mirrors the experimental data.

Regardless, a key insight that emerges from this comparison to theory is that underwhelming confinement is likely a dominant driver for explaining why the floating voltages remain below the beam energy for the magnetic field range we investigated. This result in turn invites the question as to what modifications should be made to improve the response of this device. We expand on these potential solutions in the following section.

C. Improving Beam Halter Effectiveness

We can leverage results from the model and part I of this study [5] to motivate how performance can be improved. The key premise is that it is necessary to explore strategies for improving electron confinement.

As one possible strategy, in part I of this study, we saw that as the small beam halter was moved farther away form the source, the floating voltage increased. This result may be explained by the fact that the reduction in plasma density lowers the electron collision frequency and thus increases the effective Hall parameter. In turn, the electrons are more confined and the floating voltage is higher to balance the ion and electron flux. For our application in the context of a Hall thruster, this result from Part I suggests that constructing a larger device situated farther downstream may be sufficient to yield floating potentials with enough energy to retard the ion motion. This approach has the additional advantage that the effective neutral density adjacent to the device will be lower. This has several potential benefits. First, it will reduce electron-neutral collisions and thus improve confinement. Second, the charge exchange (CEX) collision

frequency increases at higher back pressures, and any beam ions that undergo a CEX collision cannot be effectively slowed down by the beam halter, reducing its effectiveness. Third, it is possible that slow ions produced from CEX with the enhanced neutral density adjacent to the beam halter can be accelerated back towards the thruster. These ions in turn could erode thruster surfaces resulting in an additional facility effect.

As a second possible strategy, we could build a device that can produce a stronger magnetic field. As seen in both the experimental and predicted results, the floating voltage increases with field strength and thus back sputter decreases due to better confinement of electrons. With that said, a potential challenge with this approach is that our experimental measurements preliminary would suggest the response of floating potential to magnetic field is approximately linear. Achieving 200-300 V of retarding potential thus may require magnetic field strengths as high as 500 G, which is prohibitive in terms of power and thermal management to produce. This challenge may be overcome by investigating permanent magnet solutions or by potentially adopting a ferromagnetic core to concentrate flux. Indeed, in part 1 of this study, we used permanent magnets on a small scale to produce a transverse magnetic field of $\sim$ 400 G.

As a third strategy, we could attempt to reduce parasitic current to the beam halter plate. In particular, assuming that drifts are not closed represents a major factor driving low confinement. Implementing dielectric boundaries on which the field lines terminate may help improvement confinement. The resulting sheath on these surfaces would serve to electrostatic confine the electrons in the region of transverse magnetic field. Alternatively, we may explore radial magnetic field designs that lead to closed drifts– in a direct analogy to Hall effect thrusters.

VIII. Conclusion

Back sputter from high energy ions impacting downstream surfaces in the facility can deposit back on the thruster and obscure accurate erosion estimates. As Hall thrusters are scaled to higher powers, the back sputter rate grows proportionally. To attempt to mitigate this back sputter, we built and tested an electromagnetic beam halter positioned downstream of a Hall thruster. The beam halter produces a transverse magnetic field in front of a graphite plate. This reduces the electron mobility to the plate and subsequently increases the plate potential to balance the ion and electron flux. The high plate potential then generates an electric field that slows down the ions and reduces back sputter.

To test the device, we operated the H9 Hall thruster at 300 V, 15 A, and 200 V, 15 A. At both thruster conditions, we swept the solenoid current from 0 to 6 A. We measured the plate floating voltage and back sputter rate to determine the beam halter effectiveness. We monitored the thruster cathode to ground voltage to analyze the impact of the beam catcher on thruster operation. During operation, we saw that the plate floating voltage monotonically increased at all conditions with increasing beam halter magnetic field strength. This corresponded to a general decrease in back sputter. At 300 V the maximum reduction in back sputter was $\sim$ 20 % and at 200 V the maximum was $\sim$ 40 %. The greater reduction in back sputter at 200 V compared to 300 V is likely due to the non-linear dependence of the sputter yield curve on ion energy. The cathode to ground voltage changed minimally across all operating conditions ($\sim$ 3 V), indicating that the beam halter is shielded from the thruster discharge.

To help understand this performance, we compared our model predictions to the experimentally measured floating voltage. While the model captured the increase in floating voltage as a function of magnetic field, it did not accurately capture the trend. The Bohm-like form agreed better with the data, which qualitatively indicates that the transport is non-classical in the transverse region of the device. Using our model and the results from part 1, we hypothesized that to increase effectiveness, we need to reduce the plasma density to decrease the electron collision frequency and improve confinement. To accomplish this, we proposed build a bigger device positioned farther farther downstream. This has the additional advantage of a lower background pressure at the device. We also hypothesized that stronger magnetic fields could further reduce the electron mobility. We may be able to accomplish this with permanent magnets or a ferromagnetic core. Ultimately, this work demonstrated that the beam halter reduced carbon back sputter by 20-40 % without significantly impact thruster performance, and highlighted key avenues to explore to improve device effectiveness.

IX. Acknowledgments

This work was supported by the Joint Advanced Propulsion Institute, a NASA Space Technology Research Institute and a NASA Space Technology Graduate Research Opportunity (Grant: 80NSSC23K1187).

References

[1] Hofer, R. R., Jorns, B. A., Polk, J. E., Mikellides, I. G., and Snyder, J. S., "Wear test of a magnetically shielded Hall thruster at 3000 seconds specific impulse," *33rd International Electric Propulsion Conference*, 2013.

[2] Shastry, R., Herman, D. A., Soulas, G. C., and Patterson, M. J., "Status of NASA's Evolutionary Xenon Thruster (NEXT) long-duration test as of 50,000 h and 900 kg throughput," *International Electric Propulsion Conference (IEPC2013)*, 2015.

[3] Lobbia, R. B., Polk, J. E., Hofer, R. R., Chaplin, V. H., and Jorns, B., "Accelerating 23,000 hours of ground test backsputtered carbon on a magnetically shielded Hall thruster," *AIAA Propulsion and Energy 2019 Forum*, 2019.

[4] Walker, M. L., Lev, D., Saeedifard, M., Jorns, B., Foster, J., Gallimore, A. D., Gorodetsky, A., Rovey, J. L., Chew, H. B., Levin, D., Williams, J., Yalin, A., Wirz, R., Marian, J., Boyd, I., Hara, K., and Lemmer, K., "Overview of the Joint AdvaNced PropUlsion InStitute (JANUS)," *37th International Electric Propulsion Conference*, 2022.

[5] Thomson, S., Garman, J., Robertson, J., Williams, J., Hurley, W., Gill, T., Whittaker, C., and Jorns, B., "Methods for Mitigating Backsputter in Electric Propulsion Test Facilities I: Beam Halter Concept and Design," *SciTech Forum and Exposition*, 2024.

[6] Williams, J., Johnson, M., and Williams, D., "Differential sputtering behavior of pyrolytic graphite and carbon-carbon composite under xenon bombardment," *40th AIAA/ASME/SAE/ASEE Joint Propulsion Conference and Exhibit*, 2004, p. 3788.

[7] Frieman, J. D., King, S. T., Walker, M. L., Khayms, V., and King, D., "Role of a conducting vacuum chamber in the hall effect thruster electrical circuit," *Journal of Propulsion and Power*, Vol. 30, No. 6, 2014, pp. 1471–1479.

[8] Hutchinson, I. H., "Principles of plasma diagnostics," *Plasma Physics and Controlled Fusion*, 2002.

[9] Hofer, R. R., Cusson, S. E., Lobbia, R. B., and Gallimore, A. D., "The H9 Magnetically Shielded Hall Thruster," *35th International Electric Propulsion Conference*, Atlanta, GA, 2017.

[10] Cusson, S. E., Hofer, R. R., Lobbia, R., Jorns, B. A., and Gallimore, A. D., "Performance of the H9 Magnetically Shielded Hall Thrusters," *35th International Electric Propulsion Conference*, Atlanta, Georgia, 2017.

[11] Mikellides, I. G., Katz, I., Hofer, R. R., Goebel, D. M., de Grys, K., and Mathers, A., "Magnetic Sheilding of the channel walls in a Hall plasma accelerator," *Physics of Plasmas*, Vol. 18, No. 033501, 2011. https://doi.org/10.1063/1.3551583.

[12] Mikellides, I., Katz, I., Hofer, R., and Goebel, D., "Magnetic Shielding of a Laboratory Hall thruster," *Journal of Applied Physics*, Vol. 115, No. 043303, 2014. https://doi.org/10.1063/1.4862313.

[13] Viges, E. A., Jorns, B. A., Gallimore, A. D., and Sheehan, J., "University of Michigan's upgraded large vacuum test facility," *36th International Electric Propulsion Conference*, 2019.

[14] Su, L., and Jorns, B., "Performance comparison of a 9-kW magnetically shielded Hall thruster operating on xenon and krypton," *Journal of Applied Physics*, Vol. 130, No. 16, 2021.

[15] Jorns, B., and Byrne, M., "Model for the dependence of cathode voltage in a Hall thruster on facility pressure," *Plasma Sources Science and Technology*, Vol. 30, No. 1, 2021, p. 015012.

[16] Yim, J. T., "A survey of xenon ion sputter yield data and fits relevant to electric propulsion spacecraft integration," *International Electric Propulsion Conference (IEPC)*, 2017.